Atmospheric
Chemistry
and Physics

Estimation of cloud condensation nuclei concentration from aerosol optical quantities: influential factors and uncertainties

Jianjun Liu[1,2] **and Zhanqing Li**[1,2]

[1]State Laboratory of Earth Surface Process and Resource Ecology, GCESS, Beijing Normal University, Beijing, China.
[2]Department of Atmospheric and Oceanic Science and Earth System Science Interdisciplinary Center, University of Maryland, College Park, Maryland, USA

Correspondence to: Zhanqing Li (zli@atmos.umd.edu)

Abstract. Large-scale measurements of cloud condensation nuclei (CCN) are difficult to obtain on a routine basis, whereas aerosol optical quantities are more readily available. This study investigates the relationship between CCN and aerosol optical quantities for some distinct aerosol types using extensive observational data collected at multiple Atmospheric Radiation Measurement (ARM) Climate Research Facility (CRF) sites around the world. The influences of relative humidity (RH), aerosol hygroscopicity (f_{RH}) and single scattering albedo (SSA) on the relationship are analyzed. Better relationships are found between aerosol optical depth (AOD) and CCN at the Southern Great Plains (US), Ganges Valley (India) and Black Forest sites (Germany) than those at the Graciosa Island (the Azores) and Niamey (Niger) sites, where sea salt and dust aerosols dominate, respectively. In general, the correlation between AOD and CCN decreases as the wavelength of the AOD measurement increases, suggesting that AOD at a shorter wavelength is a better proxy for CCN. The correlation is significantly improved if aerosol index (AI) is used together with AOD. The highest correlation exists between CCN and aerosol scattering coefficients (σ_{sp}) and scattering AI measured in situ. The CCN–AOD (AI) relationship deteriorates with increasing RH. If RH exceeds 75 %, the relationship where AOD is used as a proxy for CCN becomes invalid, whereas a tight σ_{sp}–CCN relationship exists for dry particles. Aerosol hygroscopicity has a weak impact on the σ_{sp}–CCN relationship. Particles with low SSA are generally associated with higher CCN concentrations, suggesting that SSA affects the relationship between CCN concentration and aerosol optical quantities. It may thus be used as a constraint to reduce uncertainties in the relationship. A significant increase in σ_{sp} and decrease in CCN with increasing SSA is observed, leading to a significant decrease in their ratio (CCN/σ_{sp}) with increasing SSA. Parameterized relationships are developed for estimating CCN, which account for RH, particle size, and SSA.

1 Introduction

Aerosols play important roles in Earth's climate and the hydrological cycle via their direct and indirect effects (IPCC, 2007). Aerosol particles can scatter and absorb solar radiation, and alter the vertical distribution of solar energy and atmospheric stability (Ramanathan et al., 2001; Liu et al., 2012). These are known as direct effects. Aerosols can modify microphysical and macroscopic cloud properties, such as cloud particle size, cloud albedo (Twomey, 1977; Twomey et al., 1984; Rosenfeld et al., 2001; Andreae et al., 2004; Koren et al., 2005) and cloud-top heights (Andreae et al., 2004; Lin et al., 2006; Li et al., 2011). They can also influence warm- and cold-rain processes (Rosenfeld and Woodley, 2000; Andreae et al., 2004; Lin et al., 2006; Bell et al., 2008; Li et al., 2011), the depth of the mixed-phase region in a cloud (Andreae et al., 2004; Koren et al., 2005, 2008, 2010; Niu and Li, 2012) and the occurrence of lightning (Orville et al., 2001; Steiger and Orville, 2003; Yuan et al., 2011; Yang et al., 2013). These are known as aerosol's indirect effects, which are the largest sources of uncertainty in the forcing of Earth's climate system. Determining CCN (cloud condensation nuclei) concentrations and their spatial and temporal variations are key challenges in quantifying aerosol's indirect effects.

CCN concentration has been measured chiefly through field experiments by counting the number of droplets formed in a chamber using optical counters at various levels of water vapor supersaturation (S) (Hudson and Yum, 2002; Ross et al., 2003; Yum et al., 2007; Rose et al., 2008; Liu et al., 2011). However, such in situ measurements of CCN concentration are few and localized and thus may not represent large areas. Extensive measurements of CCN concentration are not currently feasible because of the high cost and complex nature of the operation. CCN is determined by the aerosol size distribution and chemical composition and is governed by the Köhler theory. Aerosol particles in the ambient environment are often very complex and are comprised of inorganic and organic species (Kanakidou et al., 2005; Zhang et al., 2007), so the Köhler theory has been extended to include the influence of these species (Shulman et al., 1996; Facchini et al., 1999; Svenningsson et al., 2006). The mixing state and a detailed knowledge of how different compounds interact with water also matter (McFiggans et al., 2006; Andreae and Rosenfeld, 2008; Ward et al., 2010; Yang et al., 2012). A modified Köhler theory, called the "κ-Köhler" theory, was proposed by Petter and Kriedenweis (2007), which uses a single parameter, κ, to describe the solubility effect on CCN activation.

Unlike CCN concentration and size-resolved aerosol composition, aerosol optical quantities, such as aerosol optical depth (AOD) and aerosol scattering/extinction coefficients, are much more readily available using ground-based and space-borne remote sensing instruments. Aerosol optical quantities, especially AOD, have often been used as a proxy for CCN in large-scale model simulations (Quaas et al., 2009; Wang et al., 2011; Tao et al., 2012; Grandey et al., 2013) and in studying aerosol's indirect effects (Nakajima, 2001; Bréon et al., 2002; Feingold et al., 2003; Yuan et al., 2008). However, AOD represents the vertically integrated attenuation and depends not only on the number of particles but also on relative humidity (RH), size distribution, etc., and might not be a good proxy for CCN (Jeong et al., 2007). The use of aerosol optical measurements to estimate CCN concentrations is appealing but challenging because they are governed by different aerosol attributes (Ghan et al., 2006; Kapustin et al., 2006; Andreae, 2009). Nevertheless, attempts at relating CCN concentration to AOD or aerosol extinction/scattering properties have shown gross correlations between CCN concentration and aerosol optical quantities (Ghan and Collins, 2004; Ghan et al., 2006; Shinozuka et al., 2009; Andreae, 2009; Jefferson, 2010; Liu et al., 2011). The correlation is often fraught with uncertainties that could be reduced by accounting for some influential factors, such as aerosol size and/or composition, as well as environmental variables (e.g., RH). Previous attempts have been made to try to account for the influence of RH (Ghan and Collins, 2004; Ghan et al., 2006), but few systematic investigations have been conducted (Andreae, 2009), due partially to the dearth of measurements available at the time.

Thanks to the US Department of Energy, which is responsible for the deployment of the Atmospheric Radiation Measurement (ARM) Climate Research Facility (at fixed and mobile locations), CCN and many pertinent variables have been measured in recent years, allowing for the study presented here. The goal of this study is to gain further insights into the relationship between CCN and aerosol optical quantities, such as columnar AOD and aerosol scattering coefficients, by exploiting rich ARM data acquired around the world with different background aerosol types. To reduce the uncertainty in CCN estimations from aerosol optical measurements, we investigate the influence of RH, aerosol hygroscopicity and aerosol single scattering albedo (SSA) on the relationship between CCN and aerosol optical measurements. Measurements and methods used are described in Sect. 2. Section 3 presents results from various analyses and a summary is given in Sect. 4.

2   Data and methodology

2.1   Data

ARM data from five sites are used, representing different regions (e.g., continental and marine) dominated by different types of aerosols: the US Southern Great Plains (SGP, permanent site, typical rural continental aerosols over farm land), Graciosa Island in the Azores (GRW, mobile facility site, sea salt aerosols and local pollution from airport traffic and long-range transport from Europe), the Black Forest in Germany (FKB, mobile facility, agricultural and forested regions with rich biogenic aerosols), the Ganges Valley in India (GVAX, mobile facility site, anthropogenic pollution, high concentrations of sulfate, nitrate, organic and black carbon particles), and Niamey in Niger (NIM, mobile facility site, dust aerosols). The locations and observation periods, as well as measurements used in this study, are listed in Table 1. More detailed information about each site can be found at http://www.arm.gov/sites.

AOD and the Angstrom wavelength exponent (α) data were obtained from the National Aeronautics and Space Administration's Aerosol Robotic Network (AERONET) database (Holben et al., 1998; http://aeronet.gsfc.nasa.gov). The quality and consistency of AERONET AOD data are well controlled and continuously monitored. There were no AERONET retrievals available for the FKB site. Cimel sunphotometers used in the AERONET measure direct solar and sky radiances at discrete wavelengths (340, 380, 440, 500, 670, 870, 940 and 1020 nm) from which AOD is retrieved at each wavelength with an uncertainty of 0.01–0.02 (Dubovik and King, 2000). At the FKB site, AOD and α were retrieved from the multifilter rotating shadow band radiometer (MFRSR). The MFRSR measures total and diffuse solar broadband irradiances at 415, 500, 610, 673, 870, and 940 nm with an AOD retrieval accuracy of ~ 0.01 (Alexander

Table 1. Description of ARM[1] data sets selected for this study.

Site[2]	Location/Altitude	Time range	Environment	Measurements used in the study
SGP	36.6° N, 97.5° W/320 m	2006.09–2011.04	Agricultural	AOD[3] and α[4] from AERONET[5] measurements
GRW	39.1° N, 28.0° W/15 m	2009.05–2010.12	Marine	CCN[6], CN[7], $\sigma_{sp}(\sigma_{ap})$[8], SSA[9], $f_{RH(RH/RH_{Ref})}$[10]
NIM	13.5° N, 2.2° E/205 m	2006.08–2007.01	Dust region	from ground-based AOS[11]
GVAX	29.4° N, 79.5° E/1936 m	2011.06–2012.04	Industrial emission and biomass burning	Atmospheric RH from surface meteorological instrumentation
FKB	48.5° N, 8.4° E/511 m	2007.04–2007.12	Forest	

[1] ARM Atmospheric Radiation Measurement; [2] SGP Southern Great Plains, USA; GRW Graciosa Island, Azores; NIM Niamey, Niger, West Africa; GVAX Ganges Valley Aerosol Experiment, Ganges Valley region of India; FKB Black Forest region, Germany;
[3] AOD aerosol optical depth; [4] α Angstrom wavelength exponent; [5] AERONET Aerosol Robotic Network; [6] CCN cloud condensation nuclei; [7] CN condensation nuclei;
[8] σ_{sp} aerosol light scattering coefficients; σ_{ap} aerosol light absorption coefficients; [9] SSA single scattering albedo, equal to the ratio of σ_{sp} to $(\sigma_{sp} + \sigma_{ap})$;
[10] $f_{RH(RH/RH_{Ref})}$ aerosol hygroscopic growth factor defined as the ratio of σ_{sp} at a given RH to σ_{sp} at a low reference RH; [11] AOS aerosol observing system, the primary ARM platform for in situ aerosol measurements made at the surface.

et al., 2008). The consistency of AOD and α retrieved from the Cimel sun-photometer and the MFRSR has been investigated by Lee et al. (2010). Close agreements were found at all wavelengths except at 415 nm. MFRSR-derived α used in this study was calculated using data at 500 and 675 nm.

CCN and aerosol condensation nuclei (CN) concentrations, aerosol scattering and absorption properties, as well as the aerosol hygroscopic growth factor (f_{RH}), are measured by a suite of instruments comprising the aerosol observing system (AOS), which is the primary ARM platform measuring in situ aerosol properties at the surface (Jefferson, 2011). CN concentrations are measured by the compact and rugged TSI Model 3010 instrument, which counts the number of particles with diameters in the size range of 10 nm to 3 μm. CCN concentrations are measured by the Droplet Measurement Technology (DMT) CCN counter at seven levels of supersaturation (S; Roberts and Nenes, 2005). The observation interval is 5 min at each level of S. It is calibrated at the beginning and at the end of each mobile facility deployment and annually at the SGP site (Jefferson, 2011).

Aerosol scattering coefficients (σ_{sp}) integrated over the scattering angle range of 7–170° are measured with TSI Model 3565 three-wavelength (450, 550 and 700 nm) nephelometers that separate aerosols by particle diameter for total aerosols ($D_p \leq 10$ μm) and submicrometer aerosols ($D_p \leq 1$ μm). Two nephelometers are deployed, with one serving as the "reference" that measures dry σ_{sp} and the other connected to a humidity scanning system and measuring changes in σ_{sp} with RH. The humidifier scans RH from low ($\sim 40\%$) to high ($\sim 90\%$) and back to low RH on an hourly basis. Aerosol light absorption coefficients (σ_{ap}) at 470, 528 and 660 nm are measured by a filter-based Radiances Research particle/soot absorption photometer. The 470 nm σ_{ap} was normalized to 450 nm to match the σ_{sp} measured by the nephelometer. Anderson et al. (1996) and Heintzenberg et al. (2006) have reported that the uncertainty in nephelometer-measured σ_{sp} ranges from 1 to 4 Mm^{-1} for one-minute aver-

aged data. The uncertainty also depends on the magnitudes of σ_{sp} and σ_{ap} (Jefferson et al., 2011).

The aerosol hygroscopic growth factor, f_{RH}, is a parameter commonly used to quantify the increase in aerosol scattering relative to dry scattering with changes in RH, and is defined as the ratio of the σ_{sp} at a given RH to that at a low reference RH:

$$f_{RH(RH/RH_{Ref})} = \frac{\sigma_{sp(RH)}}{\sigma_{sp(RH_{Ref})}}. \tag{1}$$

The hygroscopic growth factor at RH = 85 % and RH$_{Ref}$ = 40 % is then written as $f_{RH(85\%/40\%)}$. To calculate the RH dependence of σ_{sp}, a two-parameter empirical fit is used:

$$f_{RH} = a \times \left(1 - \frac{RH\,(\%)}{100}\right)^{-b}, \tag{2}$$

where a and b are determined from σ_{sp} measured at varying RH levels (Jefferson, 2011). RH values measured by a nephelometer have an error on the order of 10 % because the instrument sensor is not well calibrated. However, bin-averaged $f_{RH(85\%/40\%)}$ has been calculated in this study using a large amount of data, so the effects of the uncertainty on results are minor. Knowing the fitting parameters, a and b, one can estimate σ_{sp} at any ambient RH:

$$\sigma_{sp}\,(amb) = \sigma_{sp}(dry)\frac{(1 - RH_{amb}/100)^{-b}}{(1 - RH_{dry}/100)^{-b}}. \tag{3}$$

2.2 Data analysis

After matching data from multiple instruments according to observation time, they are sorted into different discrete bins in which means and standard deviations are calculated. A period void of data is excluded from subsequent analyses. CCN measurements were made at different values of S, and AOD at different wavelengths, but to easily compare our finding with the study by Andreae (2009), the data used here were

made at $S = 0.4\%$ and at 500 nm, respectively. Note that $S = 0.4\%$ is more representative of convective clouds, but is too high a value for stratiform clouds. To compensate for this, low S values ($S = 0.1\%$) were considered in deriving the general aerosol optical quantities–CCN relationship for practical applications, as presented in Sect. 3.5. CCN measured at any S is adjusted to a fixed S of 0.4 and 0.1 % through the following equation:

$$\mathrm{CCN}_s = \mathrm{N}_0(1 - \exp(-b\,S^k)), \tag{4}$$

where N_0, b and k are empirically fitted parameters (Ji and Shaw, 1998). This function describes the N_{CCN}–S relationship better than the traditional formula $\mathrm{CCN}_S = \mathrm{CS}^k$ suggested by Twomey (1959) (C and k are fitted parameters). The latter overestimates CCN concentration at large S because there is no constraint on CCN as total aerosol concentration increases. Mean fitting errors in this study are 9.5, 3.2, 6.3, 23.8 and -10.7% at SGP, GRW, NIM, GVAX and FKB sites, respectively.

3 Results

3.1 Overall correlation between aerosol optical quantities and CCN

Table 2 presents the means and standard deviations of aerosol optical quantities and CCN at all sites. The largest mean AOD occurred at the NIM site (0.39 ± 0.33), which is almost four times greater than that at other sites, and the smallest mean AOD was measured at the GRW site (0.11 ± 0.06). Mean α at these two locations (NIM: 0.47 ± 0.23, GRW: 0.75 ± 0.35) are lower than that at the other sites, indicating more influence by coarse particles (dust particles at the NIM site and sea salt at the GRW site). The largest mean α at the FKB site (1.88 ± 0.27) suggests more fine particles at this site than at the SGP and GVAX sites. Mean σ_{sp} shows that submicron particles ($D_{\mathrm{p}} \leq 1\,\mu\mathrm{m}$) play a dominant role in aerosol scattering at the SGP and FKB sites. They are responsible for nearly half of the aerosol scattering at the NIM and GVAX sites. Coarse particles with diameters $> 1\,\mu\mathrm{m}$ contribute more to aerosol scattering at the GRW site. The smallest values of SSA are found at the NIM and FKB sites (0.82 ± 0.06 and 0.85 ± 0.06, respectively). As per the values of SSA and α, significantly different aerosol types are present at these sites. SSA at the SGP and GVAX sites is similar ($\sim 0.92 \pm 0.04$) and α is on the same order. On average, there was no significant difference in the magnitude of f_{RH} between these two sites where f_{RH} is generally large, indicating the presence of more hygroscopic particles. The NIM site has the lowest f_{RH} because dust aerosols are primarily composed of insoluble components or components with low solubility, while the GRW site has the highest f_{RH} because sea salt aerosols with strong hygroscopicity dominate in this area. Mean number concentrations of CN and $\mathrm{CCN}_{0.4}$ are
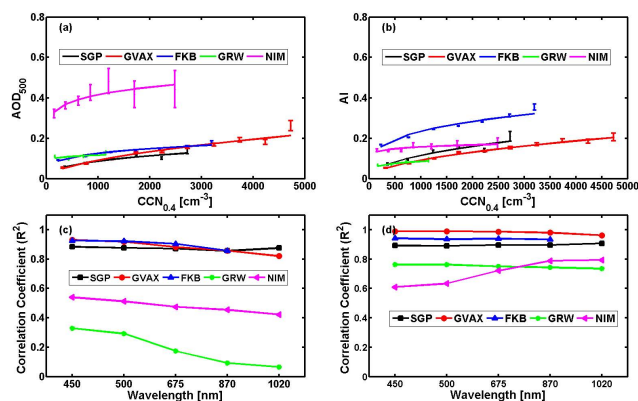

Fig. 1. (a) Relationship between AOD at 500 nm and $\mathrm{CCN}_{0.4}$, **(b)** relationship between AI and $\mathrm{CCN}_{0.4}$ **(c)** their correlation coefficients, and **(d)** same as **(c)**, but for AI in lieu of AOD.

small at the GRW site because there is less anthropogenic pollution, but the ratio of CCN to CN is high. This suggests that a large fraction of aerosol particles at this site can be activated into CCN. CN concentrations at the NIM site are the largest because dust events are frequent. The ability of dust particles to serve as CCN strongly depends on the amount of minor soluble substances contained in the dust particles (Rosenfeld et al., 2001; Kelly et al., 2007). CCN generally increases with CN during dust events, but the ratio of CCN to CN tends to decrease sharply with increasing CN, implying that less CCN become available under dusty conditions (Liu et al., 2011). This is why the smallest ratio of CCN to CN is found at the NIM site even though the $\mathrm{CCN}_{0.4}$ concentration is moderately high.

3.1.1 Relationship between columnar aerosol optical quantities and CCN

For easy comparison with Andreae (2009), AOD–CCN relationships were obtained based on the function $\mathrm{AOD} = \mathrm{a} \cdot (\mathrm{CCN}_{0.4})^b$ (Andreae, 2009) for AOD at 440, 500, 675, 870 and 1020 nm. Figure 1 presents the relationships between $\mathrm{CCN}_{0.4}$ and AOD at 500 nm (AOD_{500}), between $\mathrm{CCN}_{0.4}$ and AI, and their corresponding correlation coefficients (R^2) for different sites. AI is defined as the product of AOD_{500} and α (500–675 nm), which serves as a better proxy for CCN (Nakajima, 2001). AOD_{500} and $\mathrm{CCN}_{0.4}$ are positively correlated and the correlations are best at the SGP, GVAX and FKB sites. Although a moderate correlation exists at the NIM site, the largest standard deviations and the smallest ratio of CCN to CN representative of the site suggests that dust aerosols are not efficient CCN. They are, however, efficient in light scattering. The small value of mean α indicates that dust aerosols dominated this area during the study period. Biomass burning aerosols are also present in this area and may complicate the analysis of NIM data. The lowest correlations between $\mathrm{CCN}_{0.4}$ and

Table 2. Summary of mean aerosol optical quantities, CN concentration, and CCN concentration at 0.4 % supersaturation during the study period.

Sites	AOD 500 nm	α 500–675 nm	σ_{sp}	SSA 450 nm	f_{RH} 450 nm	CN (cm^{-3})	CCN$_{0.4}$ (cm^{-3})	CCN/CN 0.4 S
SGP	0.10 ± 0.08	1.28 ± 0.34	41.8 ± 34.1 ($D_p \leq 1\,\mu$m) 50.5 ± 44.8 ($D_p \leq 10\,\mu$m)	0.92 ± 0.05 ($D_p \leq 1\,\mu$m) 0.92 ± 0.05 ($D_p \leq 10\,\mu$m)	1.54 ± 0.28 ($D_p \leq 1\,\mu$m) 1.52 ± 0.28 ($D_p \leq 10\,\mu$m)	3944 ± 2992	1248 ± 896	0.40 ± 0.24
GRW	0.11 ± 0.06	0.75 ± 0.35	7.7 ± 7.7 ($D_p \leq 1\,\mu$m) 22.8 ± 16.5 ($D_p \leq 10\,\mu$m)	0.91 ± 0.06 ($D_p \leq 1\,\mu$m) 0.93 ± 0.04 ($D_p \leq 10\,\mu$m)	2.11 ± 0.71 ($D_p \leq 1\,\mu$m) 2.12 ± 0.57 ($D_p \leq 10\,\mu$m)	615 ± 587	287 ± 263	0.53 ± 0.30
NIM	0.39 ± 0.33	0.47 ± 0.23	54.6 ± 98.8 ($D_p \leq 1\,\mu$m) 106.2 ± 200.7 ($D_p \leq 10\,\mu$m)	0.81 ± 0.07 ($D_p \leq 1\,\mu$m) 0.82 ± 0.06 ($D_p \leq 10\,\mu$m)	1.43 ± 0.40 ($D_p \leq 1\,\mu$m) 1.14 ± 0.21 ($D_p \leq 10\,\mu$m)	5561 ± 5476	726 ± 780	0.20 ± 0.24
GVAX	0.14 ± 0.12	1.23 ± 0.45	137.9 ± 120.6 ($D_p \leq 1\,\mu$m) 218.9 ± 200.4 ($D_p \leq 10\,\mu$m)	0.92 ± 0.03 ($D_p \leq 1\,\mu$m) 0.93 ± 0.03 ($D_p \leq 10\,\mu$m)	1.66 ± 0.27 ($D_p \leq 1\,\mu$m) 1.45 ± 0.14 ($D_p \leq 10\,\mu$m)	2597 ± 1797	1426 ± 1031	0.51 ± 0.29
FKB	0.12 ± 0.05	1.88 ± 0.27	48.3 ± 35.7 ($D_p \leq 1\,\mu$m) 57.2 ± 44.3 ($D_p \leq 10\,\mu$m)	0.84 ± 0.06 ($D_p \leq 1\,\mu$m) 0.85 ± 0.06 ($D_p \leq 10\,\mu$m)	1.60 ± 0.36 ($D_p \leq 1\,\mu$m) 1.46 ± 0.25 ($D_p \leq 10\,\mu$m)	3591 ± 2098	1007 ± 749	0.29 ± 0.17

* σ_{sp} at 450 nm (Mm^{-1}); S: supersaturation.

AOD$_{500}$/AI observed at the GRW site may be attributed to sea salt aerosols. Because of their large size, their scattering may be strong relative to the low number concentration of large particles that are converted into CCN. In general, for most of the sites considered in this study, the correlation between AOD$_{500}$ and CCN deteriorates with increasing wavelength. CCN is more closely correlated with AOD measurements at shorter wavelengths because the CCN concentration is dictated by fine-mode aerosols (Andreae, 2009). The relationship varies considerably from site to site and so large errors would be incurred if one global mean relationship was used, attesting to the need of different functions for different aerosol types/regions.

Both the ability of an aerosol particle to act as a CCN at a given S level and its contribution to extinction depends on the aerosol particle size distribution. Particle size is thus also a key factor influencing the AOD–CCN relationship. To assess this potential impact, Fig. 1c and d show correlation coefficients from linear regressions of CCN$_{0.4}$ and AOD$_{500}$/AI, respectively, as a function of wavelength. Like AOD$_{500}$, AI generally increases with increasing CCN and the correlation is better than with AOD$_{500}$ at all sites. AI is more sensitive than AOD to the accumulation mode aerosol concentration, which is typically responsible for most CCN. Since α contains aerosol size information and AI conveys both aerosol loading and particle size information, the correlation between AI and CCN depends much weakly on wavelength. Compared with other pollution aerosols, dust AOD shows a slight decreasing trend with increasing wavelength, which may contribute to the slight increase in the correlation between CCN and AI at the NIM site.

3.1.2 Relationship between in situ aerosol scattering properties and CCN

Given that CCN is measured near the surface and that AOD represents total light extinction in the whole atmospheric column, the AOD–CCN relationship must be affected by the vertical distribution of aerosols. To avoid such mismatch, Fig. 2 shows results from the same analysis performed in

Table 3. Number of CCN bins and sample sizes for each bin in Figs. 2 and 4.

	SGP	GVAX	FKB	GRW	NIM
Number of bins	10	8	7	8	9
Sample size (Bin1)	57 825	1034	6585	1823	12 937
Bin2	166 278	5552	13 021	4867	9536
Bin3	173 826	3458	9008	1423	2705
Bin4	124 776	1716	3835	166	1193
Bin5	60 115	908	1113	141	604
Bin6	27 775	440	268	116	370
Bin7	13 832	210	192	116	173
Bin8	6993	136		100	196
Bin9	4385				171
Bin10	2631				

Fig. 1, but using in situ measurements of σ_{sp} at 450 nm in lieu of AOD (Fig. 2a) and the scattering aerosol index, Scat_AI (Fig. 2b). Correlation coefficients for the linear regressions of CCN$_{0.4}$ and σ_{sp} (Fig. 2c) and Scat_AI (Fig. 2d) for dry aerosol particles with $D_p \leq 1\,\mu$m as a function of wavelength are shown in Fig. 2c and d. Scat_AI is the product of σ_{sp} and the scattering wavelength exponent, α_{Scat}, which is expressed as

$$\alpha_{Scat} = -\log(\sigma_{sp,\lambda_1}/\sigma_{sp,\lambda_2})/\log(\lambda_1/\lambda_2), \qquad (5)$$

where σ_{sp,λ_1} and σ_{sp,λ_1} are scattering coefficients at wavelengths λ_1 and λ_2 (here, $\lambda_1 = 450$ nm and $\lambda_2 = 700$ nm). The number of CCN bins and sample sizes for each CCN bin are shown in Table 3. At all sites, correlations between σ_{sp} and CCN and Scat_AI and CCN are greater than those for the AOD–CCN and AI–CCN relationships (Fig. 1). The highest correlations are found for the Scat_AI–CCN relationships, which also exhibit much less wavelength dependence.

The sound relationship between aerosol optical quantities and CCN concentration indicates that if the vertical profile of aerosol scattering properties is known, the CCN profile may be estimated. Note that the ARM program has adopted the method of Ghan et al. (2006) to produce vertical profiles of CCN at its long-term sites. The method is based on
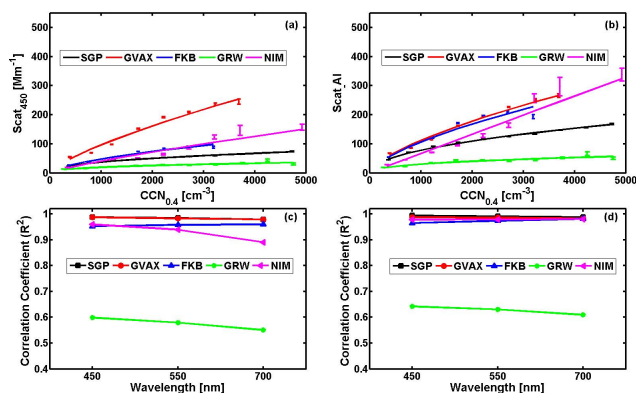
Fig. 2. Same as Fig. 1, but AOD is replaced by aerosol scattering coefficients for dry aerosol particles with diameters of less than 1 μm measured by nephelometers.

aerosol extinction profiles, as well as surface CCN measurements. While their method and ours differ significantly because they rely on different types of scattering received by active and passive sensors, the fundamental principle is the same, namely, making use of optical measurements to derive CCN. In general, scattering is much more readily measured than CCN. While this sounds encouraging, the uncertainty is large, up to a factor of two (Andreae, 2009). Accounting for some influential factors would help reduce the uncertainty.

3.1.3   Influence of ambient RH

The aerosol humidification effect is defined as the change in AOD in response to changing RH. A hygroscopic particle can swell in size through the uptake of water, which enhances its scattering efficiency and thus increases its contribution to total extinction and AOD. On the other hand, its capability of being activated to become a CCN does not depend on RH because it activates at S. This implies that changes in ambient RH can result in variations in AOD_{500} or AI, even when $CCN_{0.4}$ concentrations remain the same. As such, the relationship between CCN and AOD or σ_{sp} is affected by RH, which is qualitatively investigated in the following way.

AOD and AI data originally averaged over different CCN concentration ranges were further binned within each CCN interval according to RH range (0–35 %, 35–75 %, and 75–100 %). Figure 3 shows AOD_{500} and AI as a function of CCN concentration for these different RH bins using data from the SGP site. Both AOD_{500} and AI increase with increasing ambient RH within the same ranges of $CCN_{0.4}$ concentration. The correlation between AOD_{500} and CCN concentration becomes weak when ambient RH values are above 75 % due to the strong aerosol swelling effect on AOD_{500} (Jeong et al., 2007). The increase in particle size implies that α decreases, which has been demonstrated by others (Noh et al., 2011). This increase in AOD and decrease in α with increasing RH complicates the relationship between AI and $CCN_{0.4}$. Unless
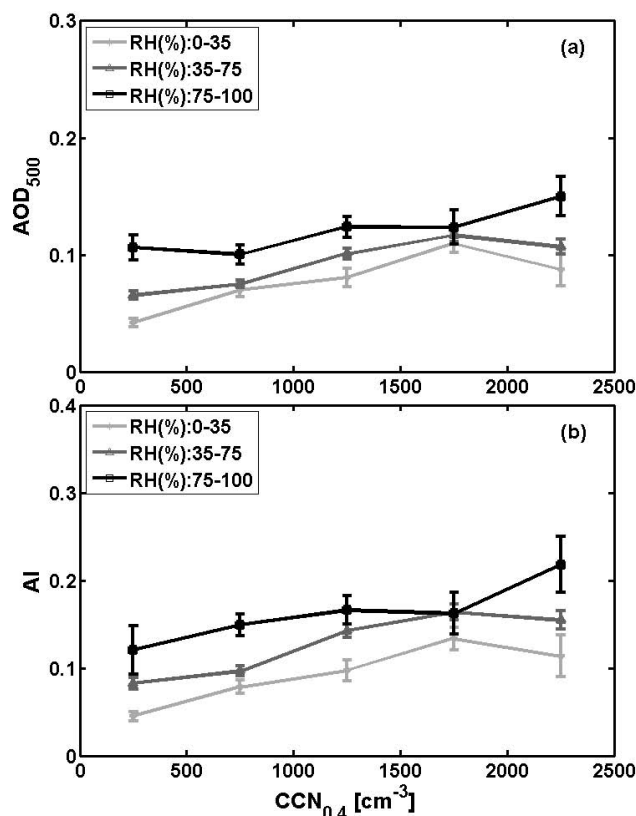

Fig. 3. (a) AOD at 500 nm and **(b)** AI as a function of $CCN_{0.4}$ concentration for different ranges of ambient RH. Data are from the SGP site.

RH is very high, e.g., greater than 95 %, changes in humidity do not influence the wavelength dependence of scattering in any significant way because scattering coefficients at all wavelengths change by similar factors and absorption is usually a minor fraction of extinction (Shinozuka et al., 2007). AOD_{500} or AI values under lower ambient RH conditions are more representative of the real effects of aerosols.

Figure 4 shows the correlation coefficients of the relationships between in situ σ_{sp} and CCN for aerosol particles with $D_p \leq 1$ μm and at ambient RH conditions as a function of wavelength at all sites. The CCN bins used are the same as in Fig. 2 and ambient σ_{sp} are averaged in each CCN bin. Aerosol σ_{sp} measurements, CCN concentrations, ambient RH measurements, and calculated aerosol hygroscopic growth factors were temporally matched. The aerosol hygroscopic growth factor is calculated at 1 h intervals. Scattering coefficients corrected for ambient RH have a temporal resolution of one minute and are matched with the closest hourly value of aerosol hygroscopic growth factor. The correlation coefficients of σ_{sp}–CCN relationships at ambient RH levels are generally lower than those under dry RH conditions (Fig. 2c). For example, at the GRW site, there is almost no relationship between $CCN_{0.4}$ and σ_{sp} at ambient conditions because particles over the site have a strong hygroscopicity.
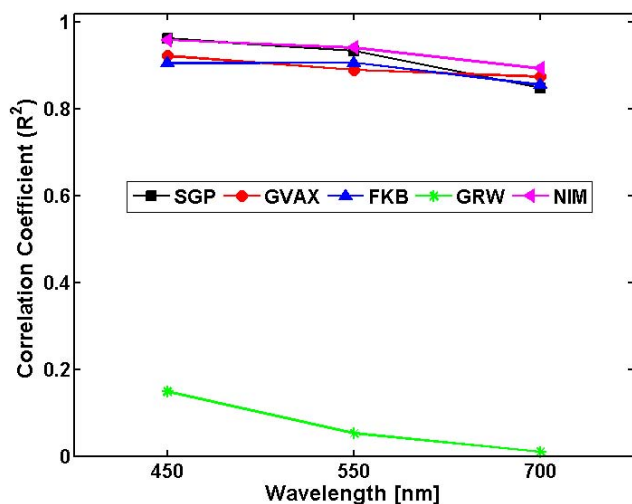
Fig. 4. Correlation coefficients of the relationship between surface-measured aerosol scattering coefficients and $CCN_{0.4}$ concentrations as a function of wavelength for ambient RH conditions and with aerosol particle diameters of less than 1 µm.

The σ_{sp}–CCN relationship at the NIM site is least affected by RH because RH is low in that region and the prevalent dust aerosols have a relatively low hygroscopicity. These results suggest that the influence of RH on the relationship between aerosol optical quantities and CCN concentration needs to be taken into consideration unless RH is low enough for humidification to be negligible.

3.1.4 Influence of aerosol hygroscopicity

Hygroscopicity and RH jointly determine the swelling effect, which affects AOD and σ_{sp}, and thus the AOD (σ_{sp})–CCN relationship. Having addressed the effect of RH, hygroscopicity is investigated by minimizing the influence of ambient RH through use of in situ measurements of σ_{sp} under fixed moderately dry conditions ($\sim 40\%$). Figure 5 shows σ_{sp}–$CCN_{0.4}$ relationships for different ranges of f_{RH} for dry aerosol particles with $D_p \leq 1$ µm (Fig. 5a) and $D_p \leq 10$ µm (Fig. 5b) at the SGP site. The sample sizes in Fig. 5a and b are given in Table 4. No clear influence of f_{RH} on any σ_{sp}–CCN relationship for dry particles with $D_p \leq 1$ µm and $D_p \leq 10$ µm is seen.

The aerosol property f_{RH} depends strongly on aerosol chemical composition (Jeong et al., 2007; Liu et al., 2011) and conveys information about the enhancement of aerosol light scattering/extinction as RH increases. Fundamentally, if aerosol particles are highly hygroscopic, they should be more readily activated into CCN. To further assess the influence of f_{RH} on the σ_{sp}–CCN relationship, the CCN concentration and σ_{sp} at 450 nm for dry particles with $D_p \leq 10$ µm (Fig. 6a) and the ratio of CCN to σ_{sp} (Fig. 6b) as a function of f_{RH} are plotted. No significant changes in CCN and σ_{sp} with increasing f_{RH} are found, especially when f_{RH} is greater than 1.5
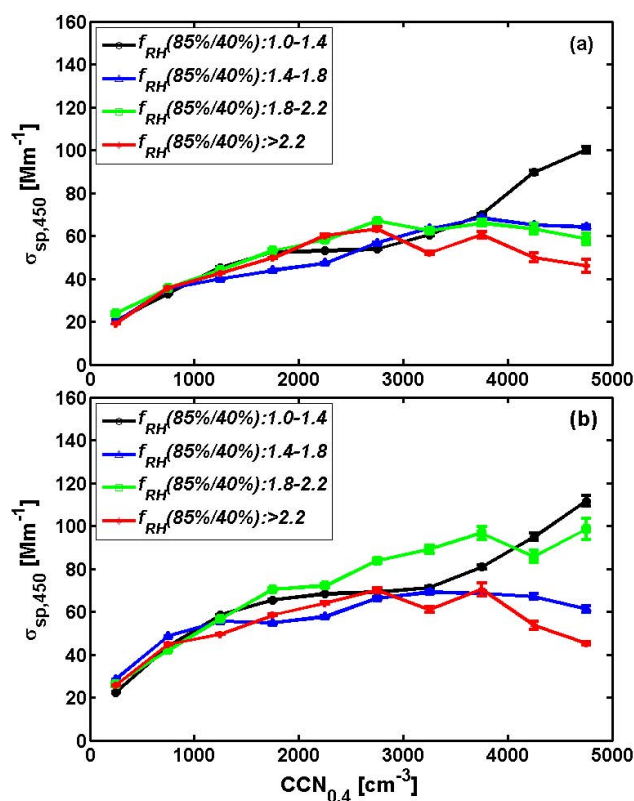

Fig. 5. Relationship between $CCN_{0.4}$ concentrations and aerosol scattering coefficients at 450 nm for dry aerosol particles with **(a)** $D_P \leq 1$ µm and **(b)** $D_P \leq 10$ µm for different ranges of aerosol hygroscopic growth factor. Data are from the SGP site.

(Fig. 6a). Since there is no significant variation in CCN and σ_{sp} with changes in f_{RH}, the ratio of CCN to σ_{sp} is insensitive to increasing f_{RH}. This supports the finding that f_{RH} has a weak influence on the σ_{sp}–CCN relationship. The scattering wavelength exponent associated with each value of f_{RH} is 1.69 ± 0.40, 1.67 ± 0.40, 1.70 ± 0.40 and 1.76 ± 0.34, respectively, which shows almost no change with variations in f_{RH}.

It is still unclear whether f_{RH} is useful for inferring CCN properties (Ervens et al., 2007). Studies have shown that the most important piece of information for CCN closure is the aerosol size distribution, followed by aerosol composition (Dusek et al., 2006). Both affect aerosol hygroscopicity (Ervens et al., 2007). As natural aerosols are usually well mixed, the true effect of chemical composition may not stand out clearly, especially if its signal is weaker than the other uncertainties. Aerosol composition at the SGP site does not vary dramatically, so f_{RH} there may be more dependent on changes in the aerosol size (Hegg et al., 1993). Mean α does change slightly in each bin, which may indicate that there are differences in aerosol composition after all. Also, α may not completely describe the aerosol particle size, especially

Table 4. Sample size for the data points in Fig. 5a and b.

Particle Size	f_{RH} Bins	CCN Bins (cm^{-3})									
		0–500	500–1000	1000–1500	1500–2000	2000–2500	2500–3000	3000–3500	3500–4000	4000–4500	4500–5000
$D_p \le 1\,\mu m$	f_{RH} (1.0–1.4)	22 833	69 685	107 688	88 531	38 563	15 220	7344	3660	2278	1344
	f_{RH} (1.4–1.8)	41 441	85 718	61 428	41 203	23 322	14 012	7551	4651	3097	1862
	f_{RH} (1.8–2.2)	25 889	53 929	35 743	24 075	11 242	5192	2044	773	389	180
	f_{RH} (> 2.2)	8258	25 190	17 361	8299	3078	1142	766	208	77	30
$D_p \le 10\,\mu m$	f_{RH} (1.0–1.4)	18 340	43 649	63 002	52 860	24 022	8007	3796	1769	872	598
	f_{RH} (1.4–1.8)	33 002	59 206	33 851	17 318	9444	5876	3418	2184	1313	962
	f_{RH} (1.8–2.2)	11 890	25 148	17 253	11 590	5572	2595	1013	516	365	153
	f_{RH} (> 2.2)	5158	13 135	10 207	6588	3540	1299	704	226	79	29
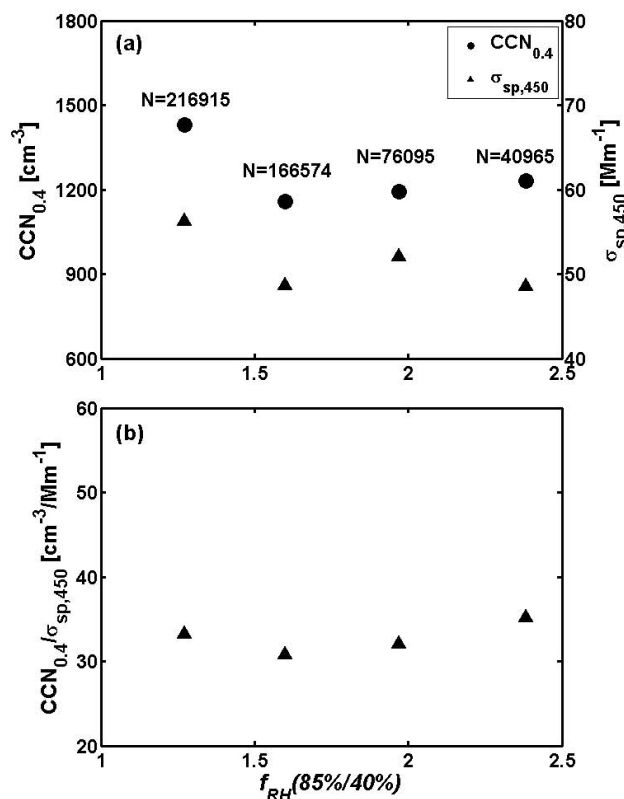
Fig. 6. (a) $CCN_{0.4}$ concentrations and aerosol scattering coefficients, and **(b)** their ratio as a function of f_{RH} for dry particles with $D_P \le 10\,\mu m$. Data are from the SGP site.

for small particles, which are not optically sensitive but are f_{RH}-sensitive.

3.1.5 Influence of aerosol SSA

In addition to AOD and α, aerosol SSA, defined as the ratio of scattering to extinction, is another independent aerosol attribute denoting aerosol composition and size. SSA can thus potentially affect the CCN–AOD (σ_{sp}) relationship. SSA can be estimated from surface measurements made by a scanning sun-photometer, such as those used in the AERONET (Dubovik and King, 2000), by a combination of direct-beam

Table 5. Sample sizes for the data points in Fig. 7.

CCN bins (cm^{-3})	SSA (0.8–0.85)	SSA (0.85–0.95)	SSA (0.95–1.0)
0–500	1342	21 614	21 218
500–1000	3989	47 059	33 114
1000–1500	3728	48 181	27 138
1500–2000	3233	37 130	14 344
2000–2500	1746	18 841	5610
2500–3000	709	9136	2149
3000–3500	419	4552	999
3500–4000	244	2484	430
4000–4500	112	1578	218
4500–5000	67	980	105

and diffuse radiation (Zhao and Li, 2007), or a combination of surface-measured total attenuation and satellite-measured atmospheric reflection (Lee et al., 2007). Since both AOD and SSA are influenced by ambient RH, only surface measured σ_{sp} and SSA at a fixed RH ($\sim = 40\,\%$) are used here to eliminate the influence of ambient RH. Figure 7 shows σ_{sp} at 450 nm as a function of $CCN_{0.4}$ for different ranges of SSA at 450 nm with $D_p \le 1\,\mu m$. Table 5 lists sample sizes. σ_{sp} generally increases with increasing SSA for the same range of $CCN_{0.4}$ concentration. Low SSA values are generally associated with high CCN concentrations, and vice versa.

Figure 8a shows $CCN_{0.4}$ concentrations, σ_{sp}, and their ratio (CCN / σ_{sp}) at 450 nm as a function of SSA for $D_p \le 1\,\mu m$. $CCN_{0.4}$ concentrations decrease slightly with increasing SSA, while σ_{sp} increases significantly with increasing SSA. Their ratio decreases significantly with increasing SSA. One explanation for these dependencies involves an air mass containing light-absorbing soot particles coated with volatile material (e.g., sulfates and organics) (Clarke et al., 2007). These particles can act as CCN, but scatter radiation poorly, therefore they have a lower SSA (Shinozuka, 2008). As they age, the particles grow in size due to deposition of soluble mass, such as sulfate and nitrate. They can then scatter more even while their number concentration remains constant or decreases due to coagulation (Shinozuka, 2008). To constrain any influence of particle size, which also affects
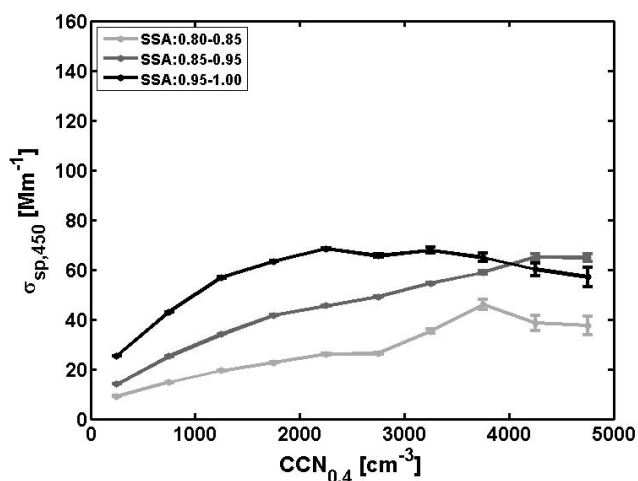
Fig. 7. Relationship between aerosol scattering coefficients at 450 nm and $CCN_{0.4}$ concentrations for different ranges of SSA and for dry particles with $D_P \leq 1\,\mu m$.
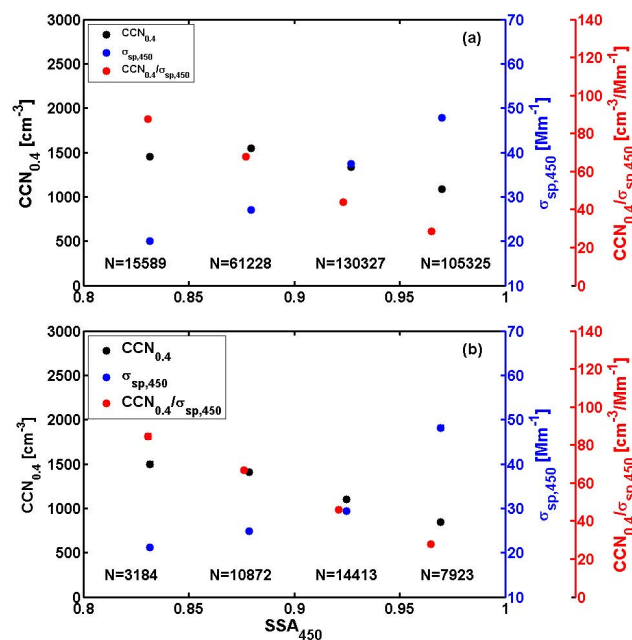

Fig. 8. $CCN_{0.4}$ concentration, aerosol scattering coefficient and their ratio as a function of SSA at 450 nm for all dry particles with $D_P \leq 1\,\mu m$ for **(a)** all values of the extinction Ångstrom exponent and **(b)** values of the extinction Ångstrom exponent that fall between 1.6 and 1.8. The sample number in each SSA bin for each case is given in each panel.

CCN and aerosol optical quantities, the same relationships as in Fig. 8a are plotted in Fig. 8b, but using only data with α ranging from 1.6 to 1.8. Similar trends are found, eliminating particle size as a driving force behind the relationships.

Results presented here suggest that SSA has a significant influence on the relationship between CCN concentration and aerosol optical quantities and if used as a constraint, may reduce uncertainties in the relationship. Similar results were reported by Shinozuka (2008), who showed that by using SSA as a constraint, the estimation of CCN concentration from aerosol extinction coefficients for pollution particles in Mexico is improved by up to 20–30 %.

3.1.6 Parameterizations for estimating CCN

The above analyses serve a guide toward developing more accurate relationships between CCN and aerosol optical properties by accounting for the major influential factors. A relationship between CCN and AOD is first developed by considering the influences of particle size and aerosol SSA. Correcting for the strong influence of RH cannot be generalized because it depends on aerosol type. On the other hand, the swelling effect is only significant for large RH ($>90\,\%$). Here, the parameterization is limited to RH $<80\,\%$, i.e., only measurements made under dry to moderately moist conditions are used. The parameterization based upon the large data set from the ARM SGP site may be valid for other rural continental regions.

The parameterization is given as

$$CCN_{0.4} = 1.2824e^5 \cdot [AOD_{500} \cdot \alpha]^{2.3941}\ 0.85 < SSA < 0.95 \quad (6)$$

R^2 is 0.94 and the mean relative error (RE), defined as $(CCN_C - CCN_M)/CCN_M$, is 0.85. CCN_C and CCN_M represent calculated CCN concentration using Eq. (6) and measured

CCN concentration, respectively. SSA is limited to 0.85–0.95, which represents most aerosol particles with moderate scattering and absorbing properties.

The relatively large error is mainly attributed to the fact that CCN is measured near the surface, but AOD represents total light extinction in the whole atmospheric column. Any unaccounted for swelling effect is not expected to be very large due to the constraint in RH. Compared to the use of a single fixed relationship between CCN and AOD, R^2 is improved by 9.3 % (0.94 vs. 0.86) and RE is improved about 11.5 % (0.85 vs. 0.96).

If there are in situ aerosol optical measurements available, such as σ_{sp} at 450 nm, estimation of CCN can be further improved by the following parameterization:

$$CCN_{0.4} = 2.3397 \cdot [\sigma_{sp} \cdot \alpha]^{1.5178}\ 0.85 < SSA < 0.95. \quad (7)$$

R^2 is improved (increasing from 0.94 to 0.99) and mean RE is reduced from 0.85 to 0.20, relative to Eq. (6). When compared to a single fixed CCN–σ_{sp} relationship that does not account for any influential factors, the R^2 from Eq. (7) does not differ considerably (0.99 vs. 0.97); the mean RE is significantly decreased by as much as 74.7 % (0.20 vs. 0.79).

As mentioned in Sect. 2.2, a CCN parameterization is also given for CCN concentrations at $S = 0.1\,\%$. Using AOD_{500}, the parameterization is

$$CCN_{0.1} = 3.4e^4 \cdot [AOD_{500} \cdot \alpha]^{2.4752}\ 0.85 < SSA < 0.95, \quad (8)$$

where $R^2 = 0.90$ and $RE = 0.91$. Using σ_{sp} at 450 nm, the parameterization is

$$CCN_{0.1} = 0.7591 \cdot \left[\sigma_{sp} \cdot \alpha\right]^{1.5621} \quad 0.85 < SSA < 0.95, \qquad (9)$$

where $R^2 = 0.99$ and $RE = 0.20$.

4   Summary and conclusions

Aerosol loading has often been used as a proxy or predictor of CCN in cloud–aerosol interaction studies due to the dearth of CCN measurements. Based on extensive measurements of aerosol optical quantities and CCN number concentrations made at different ARM Climate Research Facility sites, the relationships between aerosol optical quantities, including columnar AOD, surface-measured aerosol scattering parameters, and CCN concentrations are assessed. For the purpose of constraining and reducing the variability and uncertainties in relating aerosol optical quantities and CCN concentrations, the influences of RH, aerosol hygroscopicity and SSA are investigated using more extensive routine measurements made at the permanent ARM SGP site.

In general, mean AOD–CCN relationships at the SGP, GVAX and FKB sites show a variable degree of correlation. A weaker correlation is found at the GRW and NIM sites where relatively large particles dominate. In general, the correlation decreases as the wavelength at which AOD is measured increases. So use of AOD values measured at the shortest wavelengths is recommended. Moreover, it is better to use AI derived from AOD measurements at two wavelengths than AOD at a single wavelength because the relationship between AI and CCN is systematically better than the CCN–AOD relationship. The best predictors of CCN are in situ aerosol scattering/extinction coefficients and aerosol indices measured simultaneously with CCN.

AOD and AI are significantly influenced by ambient RH levels. The correlation between AOD (AI) and CCN becomes weak when ambient RH values are high, e.g., greater than 75 %, due to strong aerosol swelling effects on AOD. The correlation between aerosol optical quantities and CCN concentration is much tighter for dry air than for humid air. This implies that aerosol optical quantities measured at low RH are better representatives of the real effects due to aerosols. No significant influence of the aerosol hygroscopic growth factor on any CCN–σ_{sp} relationship is found. Particles with low SSA are generally associated with higher CCN concentrations for the same scattering coefficient and lower σ_{sp} values. Aerosol SSA has a significant influence on the relationship between CCN concentration and aerosol optical loading variables, and can thus be used to reduce uncertainties in the estimate of CCN. Note that both f_{RH} and SSA are related to aerosol chemical composition.

The influential factors are accounted for in developing parameterization schemes for estimating CCN from any aerosol optical property (AOD, α, and σ_{sp}). The best results are achieved by using σ_{sp} and SSA. The parameterization is valid for RH < 80 %. If the humidification function and humidity are known, one can correct for the effect to any higher values of RH.

This study reveals the potential and limitations of using aerosol optical property measurements to infer CCN concentration with a focus on the impact of ambient RH, aerosol hygroscopic response, and SSA. Further evaluation and analyses will require aerosol composition and aerosol size distribution information, together with aerosol optical parameters and meteorological parameters for each aerosol type and region.

References

Alexander, D. T. L., Crozier, P. A., and Anderson, J. R.: Brown carbon spheres in East Asian outflow and their optical properties, Science, 321, 833–836, 2008.

Anderson, B. E., Grant, W. B., Gregory, G. L., Browell, E. V., Collins, J. E., Jr., Sachse, G. W., Bagwell, D. R., Hudgins, C. H., Blake, D. R., and Blake, N. J.: Aerosols from biomass burning over the tropical South Atlantic region: Distributions and impacts, J. Geophys. Res., 101, 24117–24137, doi:10.1029/96jd00717, 1996.

Andreae, M. O.: Correlation between cloud condensation nuclei concentration and aerosol optical thickness in remote and polluted regions, Atmos. Chem. Phys., 9, 543–556, doi:10.5194/acp-9-543-2009, 2009.

Andreae, M. O. and Rosenfeld, D.: Aerosol-cloud-precipitation interactions. Part 1. The nature and sources of cloud-active aerosols, Earth-Sci. Rev., 89, 13–41, 2008.

Andreae, M. O., Rosenfeld, D., Artaxo, P., Costa, A. A., Frank, G. P., Longo, K. M., and Silva-Dias, M. A. F.: Smoking rain clouds over the Amazon, Science, 303, 1337–1342, 2004.

Bell, T. L., Rosenfeld, D., Kim, K.-M., Yoo, J.-M., Lee, M.-I., and Hahnenberger, M.: Midweek increase in U.S. summer rain and storm heights suggests air pollution invigorates rainstorms, J. Geophys. Res., 113, D02209, doi:10.1029/2007jd008623, 2008.

Bréon, F.-M., Tanré, D., and Generoso, S.: Aerosol effect on cloud droplet size monitored from satellite, Science, 295, 834–838, 2002.

Clarke, A., McNaughton, C., Kapustin, V., Shinozuka, Y., Howell, S., Dibb, J., Zhou, J., Anderson, B., Brekhovskikh, V., Turner, H., and Pinkerton, M.: Biomass burning and pollution aerosol over North America: Organic components and their influence on spectral optical properties and humidification response, J. Geophys. Res., 112, D12S18, doi:10.1029/2006jd007777, 2007.

Dubovik, O. and King, M. D.: A flexible inversion algorithm for retrieval of aerosol optical properties from sun and sky radiance measurements, J. Geophys. Res., 105, 20673–20696, 2000.

Dusek, U., Frank, G. P., Hildebrandt, L., Curtius, J., Schneider, J., Walter, S., Chand, D., Drewnick, F., Hings, S., Jung, D., Borrmann, S., and Andreae, M. O.: Size matters more than chemistry for cloud-nucleating ability of aerosol particles, Science, 312, 1375–1378, 2006.

Ervens, B., Cubison, M., Andrews, E., Feingold, G., Ogren, J. A., Jimenez, J. L., DeCarlo, P., and Nenes, A.: Prediction of cloud condensation nucleus number concentration using measurements of aerosol size distributions and composition and light scattering enhancement due to humidity, J. Geophys. Res., 112, D10S32, doi:10.1029/2006jd007426, 2007.

Facchini, M. C., Mircea, M., Fuzzi, S., and Charlson, R. J.: Cloud albedo enhancement by surface-active organic solutes in growing droplets, Nature, 401, 257–259, 1999.

Feingold, G., Eberhard, W. L., Veron, D. E., and Previdi, M.: First measurements of the Twomey indirect effect using ground-based remote sensors, Geophys. Res. Lett., 30, 1287, doi:10.1029/2002gl016633, 2003.

Ghan, S. J. and Collins, D. R.: Use of in situ data to test a Raman lidar–based cloud condensation nuclei remote sensing method, J. Atmos. Ocean. Tech., 21, 387–394, 2004.

Ghan, S. J., Rissman, T. A., Elleman, R., Ferrare, R. A., Turner, D., Flynn, C., Wang, J., Ogren, J., Hudson, J., Jonsson, H. H., VanReken, T., Flagan, R. C., and Seinfeld, J. H.: Use of in situ cloud condensation nuclei, extinction, and aerosol size distribution measurements to test a method for retrieving cloud condensation nuclei profiles from surface measurements, J. Geophys. Res., 111, D05S10, doi:10.1029/2004jd005752, 2006.

Grandey, B. S., Stier, P., and Wagner, T. M.: Investigating relationships between aerosol optical depth and cloud fraction using satellite, aerosol reanalysis and general circulation model data, Atmos. Chem. Phys., 13, 3177–3184, doi:10.5194/acp-13-3177-2013, 2013.

Hegg, D. A., Ferek, R. J., and Hobbs, P. V.: Light scattering and cloud condensation nucleus activity of sulfate aerosol measured over the northeast Atlantic Ocean, J. Geophys. Res., 98, 14887–14894, doi:10.1029/93JD01615, 1993.

Heintzenberg, J., Wiedensohler, A., Tuch, T. M., Covert, D. S., Sheridan, P., Ogren, J. A., Gras, J., Nessler, R., Kleefeld, C., Kalivitis, N., Aaltonen, V., Wilhelm, R. T., and Havlicek, M.: Intercomparisons and aerosol calibrations of 12 commercial integrating nephelometers of three manufacturers, J. Atmos. Ocean. Tech., 23, 902–914, doi:10.1175/jtech1892.1, 2006.

Holben, B. N., Eck, T. F., Slutsker, I., Tanré, D., Buis, J. P., Setzer, A., Vermote, E., Reagan, J. A., Kaufman, Y. J., Nakajima, T., Lavenu, F., Jankowiak, I., and Smirnov, A.: AERONET – a federated instrument network and data archive for aerosol characterization, Remote Sens. Environ., 66, 1–16, 1998.

Hudson, J. G. and Yum, S. S.: Cloud condensation nuclei spectra and polluted and clean clouds over the Indian Ocean, J. Geophys. Res., 107, 8022, doi:10.1029/2001jd000829, 2002.

IPCC: Climate Change 2007: The Physical Science Basis. Contribution of Working Group I to the Fourth Assessment Report of the Intergovernmental Panel on Climate Change, Cambridge University Press, Cambridge, United Kingdom and New York, NY, USA, 2007.

Jefferson, A.: Empirical estimates of CCN from aerosol optical properties at four remote sites, Atmos. Chem. Phys., 10, 6855–6861, doi:10.5194/acp-10-6855-2010, 2010.

Jefferson, A.: Aerosol observing system (AOS) handbook, ARMTR-014, US Dep. of Energy, Washington, D. C., 2011.

Jeong, M.-J., Li, Z., Andrews, E., and Tsay, S.-C.: Effect of aerosol humidification on the column aerosol optical thickness over the Atmospheric Radiation Measurement Southern Great Plains site, J. Geophys. Res., 112, D10202, doi:10.1029/2006jd007176, 2007.

Ji, Q. and Shaw, G. E.: On supersaturation spectrum and size distributions of cloud condensation nuclei, Geophys. Res. Lett., 25, 1903–1906, 1998.

Kanakidou, M., Seinfeld, J. H., Pandis, S. N., Barnes, I., Dentener, F. J., Facchini, M. C., Van Dingenen, R., Ervens, B., Nenes, A., Nielsen, C. J., Swietlicki, E., Putaud, J. P., Balkanski, Y., Fuzzi, S., Horth, J., Moortgat, G. K., Winterhalter, R., Myhre, C. E. L., Tsigaridis, K., Vignati, E., Stephanou, E. G., and Wilson, J.: Organic aerosol and global climate modelling: a review, Atmos. Chem. Phys., 5, 1053–1123, doi:10.5194/acp-5-1053-2005, 2005.

Kapustin, V. N., Clarke, A. D., Shinozuka, Y., Howell, S., Brekhovskikh, V., Nakajima, T., and Higurashi, A.: On the determination of a cloud condensation nuclei from satellite: Challenges and possibilities, J. Geophys. Res., 111, D04202, doi:10.1029/2004jd005527, 2006.

Kelly, J. T., Chuang, C. C., and Wexler, A. S.: Influence of dust composition on cloud droplet formation, Atmos. Environ., 41, 2904–2916, 2007.

Koren, I., Kaufman, Y. J., Rosenfeld, D., Remer, L. A., and Rudich, Y.: Aerosol invigoration and restructuring of Atlantic convective clouds, Geophys. Res. Lett., 32, L14828, doi:10.1029/2005gl023187, 2005.

Koren, I., Martins, J. V., Remer, L. A., and Afargan, H.: Smoke invigoration versus inhibition of clouds over the Amazon, Science, 321, 946–949, doi:10.1126/science.1159185, 2008.

Koren, I., Feingold, G., and Remer, L. A.: The invigoration of deep convective clouds over the Atlantic: aerosol effect, meteorology or retrieval artifact?, Atmos. Chem. Phys., 10, 8855–8872, doi:10.5194/acp-10-8855-2010, 2010.

Lee, K. H., Li, Z., Wong, M. S., Xin, J., Wang, Y., Hao, W.-M., and Zhao, F.: Aerosol single scattering albedo estimated across China from a combination of ground and satellite measurements, J. Geophys. Res., 112, D22S15, doi:10.1029/2007jd009077, 2007.

Lee, K. H., Li, Z., Cribb, M. C., Liu, J., Wang, L., Zheng, Y., Xia, X., Chen, H., and Li, B.: Aerosol optical depth measurements in eastern China and a new calibration method, J. Geophys. Res., 115, D00K11, doi:10.1029/2009JD012812, 2010.

Li, Z., Niu, F., Fan, J., Liu, Y., Rosenfeld, D., and Ding, Y.: Long-term impacts of aerosols on the vertical development of clouds and precipitation, Nat. Geosci., 4, 888–894, 2011.

Lin, J. C., Matsui, T., Pielke, R. A., and Kummerow, C.: Effects of biomass-burning-derived aerosols on precipitation and clouds in the Amazon Basin: A satellite-based empirical study, J. Geophys. Res., 111, D19204, doi:10.1029/2005jd006884, 2006.

Liu, J., Zheng, Y., Li, Z., and Cribb, M. C.: Analysis of cloud condensation nuclei properties at a polluted site in southeastern China during the AMF-China Campaign, J. Geophys. Res., 116, D00K35, doi:10.1029/2011jd016395, 2011.

Liu, J., Zheng, Y., Li, Z., Flynn, C., and Cribb, M. C.: Seasonal variations of aerosol optical properties, vertical distribution and associated radiative effects in the Yangtze Delta region of China, J. Geophys. Res., 117, D00K38, doi:10.1029/2011jd016490, 2012.

Liu, P. F., Zhao, C. S., Göbel, T., Hallbauer, E., Nowak, A., Ran, L., Xu, W. Y., Deng, Z. Z., Ma, N., Mildenberger, K., Henning, S., Stratmann, F., and Wiedensohler, A.: Hygroscopic properties of aerosol particles at high relative humidity and their diurnal variations in the North China Plain, Atmos. Chem. Phys., 11, 3479–3494, doi:10.5194/acp-11-3479-2011, 2011.

McFiggans, G., Artaxo, P., Baltensperger, U., Coe, H., Facchini, M. C., Feingold, G., Fuzzi, S., Gysel, M., Laaksonen, A., Lohmann, U., Mentel, T. F., Murphy, D. M., O'Dowd, C. D., Snider, J. R., and Weingartner, E.: The effect of physical and chemical aerosol properties on warm cloud droplet activation, Atmos. Chem. Phys., 6, 2593–2649, doi:10.5194/acp-6-2593-2006, 2006.

Nakajima, T.: A possible correlation between satellite-derived cloud and aerosol microphysical parameters, Geophys. Res. Lett., 28, 1171–1174, 2001.

Niu, Feng and Li, Zhanqing: Systematic variations of cloud top temperature and precipitation rate with aerosols over the global tropics, Atmos. Chem. Phys., 12, 8491–8498, doi:10.5194/acp-12-8491-2012, 2012.

Noh, Y. M., Müller, D., Mattis, I., Lee, H., and Kim, Y. J.: Vertically resolved light-absorption characteristics and the influence of relative humidity on particle properties: Multiwavelength Raman lidar observations of East Asian aerosol types over Korea, J. Geophys. Res., 116, D06206, doi:10.1029/2010jd014873, 2011.

Orville, R. E., Huffines, G., Nielsen-Gammon, J., Zhang, R., Ely, B., Steiger, S., Phillips, S., Allen, S., and Read, W.: Enhancement of cloud-to-ground lightning over Houston, Texas, Geophys. Res. Lett., 28, 2597–2600, doi:10.1029/2001gl012990, 2001.

Petters, M. D. and Kreidenweis, S. M.: A single parameter representation of hygroscopic growth and cloud condensation nucleus activity, Atmos. Chem. Phys., 7, 1961–1971, doi:10.5194/acp-7-1961-2007, 2007.

Quaas, J., Ming, Y., Menon, S., Takemura, T., Wang, M., Penner, J. E., Gettelman, A., Lohmann, U., Bellouin, N., Boucher, O., Sayer, A. M., Thomas, G. E., McComiskey, A., Feingold, G., Hoose, C., Kristjánsson, J. E., Liu, X., Balkanski, Y., Donner, L. J., Ginoux, P. A., Stier, P., Grandey, B., Feichter, J., Sednev, I., Bauer, S. E., Koch, D., Grainger, R. G., Kirkevåg, A., Iversen, T., Seland, Ø., Easter, R., Ghan, S. J., Rasch, P. J., Morrison, H., Lamarque, J.-F., Iacono, M. J., Kinne, S., and Schulz, M.: Aerosol indirect effects – general circulation model intercomparison and evaluation with satellite data, Atmos. Chem. Phys., 9, 8697–8717, doi:10.5194/acp-9-8697-2009, 2009.

Ramanathan, V., Crutzen, P. J., Kiehl, J. T., and Rosenfeld, D.: Aerosols, climate, and the hydrological cycle, Science, 294, 2119–2124, doi:10.1126/science.1064034, 2001.

Roberts, G. C. and Nenes, A.: A continuous-flow streamwise thermal-gradient CCN chamber for atmospheric measurements, Aerosol Sci. Tech., 39, 206–221, doi:10.1080/027868290913988, 2005.

Rose, D., Gunthe, S. S., Mikhailov, E., Frank, G. P., Dusek, U., Andreae, M. O., and Pöschl, U.: Calibration and measurement uncertainties of a continuous-flow cloud condensation nuclei counter (DMT-CCNC): CCN activation of ammonium sulfate and sodium chloride aerosol particles in theory and experiment, Atmos. Chem. Phys., 8, 1153–1179, doi:10.5194/acp-8-1153-2008, 2008.

Rosenfeld, D. and Woodley, W. L.: Deep convective clouds with sustained super cooled liquid water down to −37.5 °C, Nature, 405, 440–442, 2000.

Rosenfeld, D., Rudich, Y., and Lahav, R.: Desert dust suppressing precipitation: A possible desertification feedback loop, P. Natl. Acad. Sci., 98, 5975–5980, 2001.

Ross, K. E., Piketh, S. J., Bruintjes, R. T., Burger, R. P., Swap, R. J., and Annegarn, H. J.: Spatial and seasonal variations in CCN distribution and the aerosol-CCN relationship over southern Africa, J. Geophys. Res., 108, 8481, doi:10.1029/2002jd002384, 2003.

Shinozuka, Y.: Relations between cloud condensation nuclei and aerosol optical properties relevant to remote sensing, PhD thesis, Dep. of Ocean and Earth Science and Technology, University of Hawaii at Manoa, Hawaii, US, 2008.

Shinozuka, Y., Clarke, A. D., Howell, S. G., Kapustin, V. N., McNaughton, C. S., Zhou, J., and Anderson, B. E.: Aircraft profiles of aerosol microphysics and optical properties over North America: Aerosol optical depth and its association with $PM_{2.5}$ and water uptake, J. Geophys. Res., 112, D12S20, doi:10.1029/2006jd007918, 2007.

Shinozuka, Y., Clarke, A. D., DeCarlo, P. F., Jimenez, J. L., Dunlea, E. J., Roberts, G. C., Tomlinson, J. M., Collins, D. R., Howell, S. G., Kapustin, V. N., McNaughton, C. S., and Zhou, J.: Aerosol optical properties relevant to regional remote sensing of CCN activity and links to their organic mass fraction: airborne observations over Central Mexico and the US West Coast during MILAGRO/INTEX-B, Atmos. Chem. Phys., 9, 6727–6742, doi:10.5194/acp-9-6727-2009, 2009.

Shulman, M. L., Jacobson, M. C., Carlson, R. J., Synovec, R. E., and Young, T. E.: Dissolution behavior and surface tension effects of organic compounds in nucleating cloud droplets, Geophys. Res. Lett., 23, 277–280, doi:10.1029/95gl03810, 1996.

Steiger, S. M. and Orville, R. E.: Cloud-to-ground lightning enhancement over Southern Louisiana, Geophys. Res. Lett., 30, 1975, doi:10.1029/2003gl017923, 2003.

Svenningsson, B., Rissler, J., Swietlicki, E., Mircea, M., Bilde, M., Facchini, M. C., Decesari, S., Fuzzi, S., Zhou, J., Mønster, J., and Rosenørn, T.: Hygroscopic growth and critical supersaturations for mixed aerosol particles of inorganic and organic compounds of atmospheric relevance, Atmos. Chem. Phys., 6, 1937–1952, doi:10.5194/acp-6-1937-2006, 2006.

Tao, W.-K., Chen, J.-P., Li, Z., Wang, C., and Zhang, C.: Impact of aerosols on convective clouds and precipitation, Rev. Geophys., 50, RG2001, doi:10.1029/2011rg000369, 2012.

Twomey, S.: The nuclei of natural cloud formation part II: The supersaturation in natural clouds and the variation of cloud droplet concentration, Pure Appl. Geophys., 43, 243–249, 1959.

Twomey, S.: The influence of pollution on the shortwave albedo of clouds, J. Atmos. Sci., 34, 1149–1152, 1977.

Twomey, S. A., Piepgrass, M., and Wolfe, T. L.: An assessment of the impact of pollution on global cloud albedo, Tellus B, 36, 356–366, doi:10.1111/j.1600-0889.1984.tb00254.x, 1984.

Wang, M., Ghan, S., Ovchinnikov, M., Liu, X., Easter, R., Kassianov, E., Qian, Y., and Morrison, H.: Aerosol indirect effects in a multi-scale aerosol-climate model PNNL-MMF, Atmos. Chem. Phys., 11, 5431–5455, doi:10.5194/acp-11-5431-2011, 2011.

Ward, D. S., Eidhammer, T., Cotton, W. R., and Kreidenweis, S. M.: The role of the particle size distribution in assessing aerosol composition effects on simulated droplet activation, Atmos. Chem. Phys., 10, 5435–5447, doi:10.5194/acp-10-5435-2010, 2010.

Yang, F., Xue, H., Deng, Z., Zhao, C., and Zhang, Q.: A closure study of cloud condensation nuclei in the North China Plain using droplet kinetic condensational growth model, Atmos. Chem. Phys., 12, 5399–5411, doi:10.5194/acp-12-5399-2012, 2012.

Yang, X., Yao, Z. Li, Z. and Fan. T.: Heavy air pollution suppresses summer thunderstorms in central China, J. Atmos. Sol.-Terr. Phy., 95–96, 28–40, 2013.

Yuan, T., Li, Z., Zhang, R., and Fan, J.: Increase of cloud droplet size with aerosol optical depth: an observation and modeling study, J. Geophys. Res., 113, D04201, doi:10.1029/2007JD008632, 2008.

Yuan, T., Remer, L. A., Pickering, K. E., and Yu, H.: Observational evidence of aerosol enhancement of lightning activity and convective invigoration, Geophys. Res. Lett., 38, L04701, doi:10.1029/2010gl046052, 2011.

Yum, S. S., Roberts, G., Kim, J. H., Song, K., and Kim, D.: Submicron aerosol size distributions and cloud condensation nuclei concentrations measured at Gosan, Korea, during the Atmospheric Brown Clouds and East Asian Regional Experiment 2005, J. Geophys. Res., 112, D22S32, doi:10.1029/2006jd008212, 2007.

Zhang, Q., Jimenez, J. L., Canagaratna, M. R., Allan, J. D., Coe, H., Ulbrich, I., Alfarra, M. R., Takami, A., Middlebrook, A. M., Sun, Y. L., Dzepina, K., Dunlea, E., Docherty, K., DeCarlo, P. F., Salcedo, D., Onasch, T., Jayne, J. T., Miyoshi, T., Shimono, A., Hatakeyama, S., Takegawa, N., Kondo, Y., Schneider, J., Drewnick, F., Borrmann, S., Weimer, S., Demerjian, K., Williams, P., Bower, K., Bahreini, R., Cottrell, L., Griffin, R. J., Rautiainen, J., Sun, J. Y., Zhang, Y. M., and Worsnop, D. R.: Ubiquity and dominance of oxygenated species in organic aerosols in anthropogenically-influenced Northern Hemisphere mid-latitudes, Geophys. Res. Lett., 34, L13801, doi:10.1029/2007gl029979, 2007.

Zhao, F. and Li, Z.: Estimation of aerosol single scattering albedo from solar direct spectral radiance and total broadband irradiances measured in China, J. Geophys. Res., 112, 1–10, 2007.